**Solar Polar Magnetic Fields and M8+ Earthquakes**

Ben Davidson[1], C. Wells[2], C. Guo[3]

[1] SpaceWeatherNews, 87120, Albuquerque, New Mexico
[2] UCLA, Institute for Digital Research and Education, Los Angeles, California
[3] Precision Consulting, LLC, 10003, New York, New York

Corresponding Author: Ben Davidson (Ben@ObservatoryProject.com)

Key Points:

1) The peaks in strength, and reversals of polarity, in the solar polar magnetic fields are assessed for temporal correlation with M8+ earthquakes.
2) Multiple significant correlations were found based on 10,000 simulations (>99$^{th}$ percentile) and 100,000 simulations (>99$^{th}$ percentile).
3) Evidence exists for potential exogenous modulation of earthquake processes.

## Abstract

The largest earthquakes represent one of the greatest threats to human life and infrastructure in the field of natural disasters, and yet it is considered wholly separate from the field of space weather. The subject of electromagnetic pre-seismic signals is one of considerable importance and debate in existing literature. The maximum magnetism and reversals of polarity in the solar polar magnetic fields were analyzed to determine the existence of a relationship with large earthquakes. The proximity of earth's M8+ seismic events to the times of peak magnetism and reversals of the fields were found to be significantly closer than expected based on 10,000 simulations (>$99^{th}$ percentile), with the correlation for the largest magnitude events (M8.6+) exceeding $3\sigma$ (>$99.9^{th}$ percentile) based on 100,000 simulations. Potential mechanisms are discussed, along with the potential for expansion of the scope of space weather research.


## Plain Language Summary

Numerous recent studies have shown that earthquakes often have electromagnetic pre-earthquake processes. The primary electromagnetic influence on earth is the sun, and recent studies have also tied solar phenomena to earthquakes. In this study, the sun's magnetic fields, which reach the outer solar system and can directly connect with earth's magnetic field, are shown to significantly influence the occurrence of the largest earthquakes (M8+). The times of maximum strength of the sun's fields, and their reversals of polarity (+/-), have a better correlation than more than 99% of simulations, indicating a strong likelihood that there may be a correlation between the largest earthquakes and the sun's magnetic fields.

## 1.0 Introduction

The destructive power of M8+ earthquakes underscores the importance of studying the environmental changes prior to their rupture. In recent years, dozens of studies have analyzed atmospheric or lithospheric electromagnetic anomalies near or above the epicenters of large earthquakes, including signals in outgoing longwave radiation, total electron content, GPS signals, radon and other ion emission from the ground, magnetic field ULF/VLF resonance and other geophysical parameters (Ouzounov et al., 2018). Despite the well-known fact that the sun is the primary electromagnetic actor on the earth, these processes are generally considered to be separate from the processes of space weather.

Electromagnetic pre-seismic anomalies in geospace have been reported as well (Midya and Gole, 2014; Odintsov et al., 2006; Simpson, 1967; Tavares and Azevedo, 2011). However, doubt has also been cast on a relationship between the sun and earthquakes (Guglielmi and Potapov, 2018; Love and Thomas, 2013). Numerous studies in the last few years support the existence of a correlation between seismicity and solar/geomagnetic indices, including some outside of the scope of previous works. (Cataldi et al., 2017; Elfaki and Yousef, 2017; Freund et al. 2017; Hagen and Azevedo, 2017; Larocca, 2016; Marchetti and Akhoondzadeh, 2018; Midya et al., 2016; Sukma and Abidin 2017; Urata et al., 2018; Velichkova and Kilafarska, 2018; Yu et al., 2017). Their findings illustrate need for clarity in the field, and the potential for interaction and coupling between the magnetosphere, ionosphere, atmosphere, lithosphere, global electric circuit and geomagnetic system, forming the rational basis for investigation of exogenous electromagnetic conditions and earthquake processes.

In 2015, a temporal relationship was discovered between the solar polar magnetic fields (SPF) and M8+ earthquakes; the largest seismic events tended to occur more-often during peaks of SPF magnetic strength and the reversals of SPF polarity (Davidson et al., 2015). Since that time, new SPF data has become available, more M8+ earthquakes have occurred, and both official datasets ("SPF data" and "M8+ earthquake events") used in the initial study have been altered slightly or corrected by the maintaining agencies and organizations.

With the supporting trend in the field, the availability of new data, and the open question as to the existence of the SPF-earthquake relationship given the changes to the original datasets, that relationship merits re-examination here.

## 2.0 Data Description

The data sets used in this study are freely available and regularly updated by the USGS/NCEI and the Wilcox Solar Observatory, Stanford University.

The earthquake data was accessed via the USGS government data portal found at the website address: https://earthquake.usgs.gov/earthquakes/search/ (USGS). Magnitude 8 and higher earthquakes were selected, occurring since the start of the SPF data collection, which began in May 1976. There were 33 M8+ earthquakes from the start of the data set through July 20, 2018. (USGS)

The SPF data is measured and maintained by Stanford University's Wilcox Solar Observatory and is available at the website address: http://wso.stanford.edu/Polar.html (Stanford). The north polar fields (N) and south polar fields (S) were used in this study, along with the total SPF magnetism, found by adding the north and south polar fields (N+S), which can also be accessed on a single resource (Jupyter).

### 2.1 SPF Data Oscillations and Phases

The SPF variation over time is comprised of two cyclical components, with ~11- and ~1-year oscillations matching the sunspot/solar magnetic cycle and earth's heliographic orbital variability, respectively. The SPF reverse during each sunspot maximum period of the ~11-year sunspot cycle and have an inverse strength relationship with sunspot number. Due to earth's orbital tilt stretching to ~7 degrees above and below the solar equator over the year, earth is more-exposed to one polar set of fields, oscillating every 6 months. The full N, S and N+S SPF data is presented in figure 1.

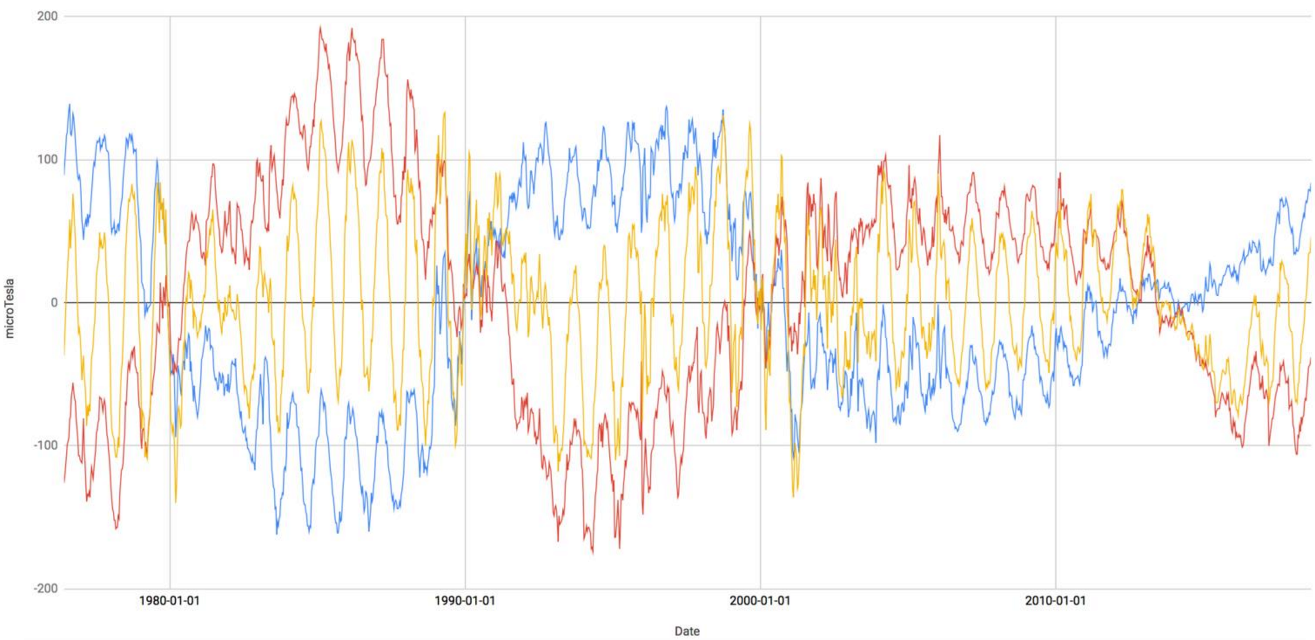


Figure 1: The 1- and 11-year oscillatory components of the north (blue) and south (red) SPF, along with the total (yellow) SPF curve. Y-axis measured in μG. Data is the complete SPF dataset, May 31, 1976 through July 10, 2018.

The "total SPF" magnetism (N+S) to which earth is subject during the 1-year oscillations normally contain a positive and a negative peak, each separated by a reversal (+/-) of the N+S SPF. Since the data is presented in 10-day averaged sets, the reversal date is considered to be the date between the 10-day marks, such that if the N+S reversed polarity from the 1st (+) to the 11th (-) of a month, the 6th would be considered the day of reversal.

The use of standard sunspot cycles to differentiate phases in the 11-year SPF oscillation is unsuitable because (1) sunspot cycles renew in the middle of the peak and largest fluctuations of the SPF, and (2) SPF reversals occur during sunspot maxima. In Davidson et al., 2015, the periods were separated based on the reversal periods of the north and south SPF, whereby the "SPF reversal" (minimum) period began during the declining phase of the 11-year SPF cycle, at the time when both north and south SPF have their first polarity reversal of that 11-year cycle. This phase ends when both poles have finished reversing in the ascending (magnitude) phase of the 11-year SPF cycle. The period outside the SPF reversal phase, which contains the maximum SPF values, is referred to as "SPF maximum". During SPF reversal the peaks are smaller, peaks *and* reversals are more frequent (less rare), and their oscillations are less predictable and less in in-sync with earth's heliographic orbital position. For 30 of the 33 M8+ earthquakes in the dataset, including the largest five events (M8.6+), the SPF were in maximum phase as opposed to reversal (minimum) phase. For these reasons, the SPF maximum period is analyzed independently here, whereby the SPF reversal phases of the 11-year SPF period shall contain no data points where M8+ earthquakes are "expected" by the model except for the phase change days themselves (the first and last days of the phase).

## 3.0 Methods

Maximum SPF force is modeled as a contributor to electromagnetic effects on large (100-1000 km) scales with lithospheric access via geomagnetic and global electric circuit pathways. SPF reversals are modeled here as when the "push" becomes a "pull", when attraction becomes repulsion in the system, or vice versa.

### 3.1 "Significant SPF Days"

The "significant SPF day(s)" include 1) total (N+S) SPF peaks occurring in SPF maximum phase, 2) total (N+S) SPF reversals occurring in SPF maximum phase, and 3) SPF phase change days.

The identification of the SPF data points in the model were done by Python code and confirmed by hand (manually) in duplicate. Mathematical identification of the significant SPF days was done using Python 2.7 and is available for download (Jupyter). Determining the "significant SPF days" in the model first requires separating SPF phases. SPF reversal periods in the dataset are: 1) 3 September 1979 to 30 May 1980, 2) 21 August 1989 to 2 June 1991, 3) 27 November 1999 to 29 June 2001, and 4) 27 May 2013 to 7 January 2015. SPF maximum occurs outside of these times. By code, N+S reversals were identified by finding all times N+S SPF underwent a sign change, going from either positive to negative or negative to positive. These dates were then filtered to only contain those dates in a SPF maximum period as determined by the dates found in the first step. Finally, since all reversals had a start and end point ten days apart, the middle day, five days between each pair of dates in a reversal was chosen as the significant point. Total (N+S) SPF peaks were identified as the date of the greatest magnitude (+ or -) of total (N+S) SPF between two N+S reversals. For a N+S peak to be significant it has to occur during a SPF maximum period and be between N+S reversals that were twenty days apart. There were a total of 213 significant SPF days out of 1540 data points. An example of the end result of this process is visualized in figure 2.

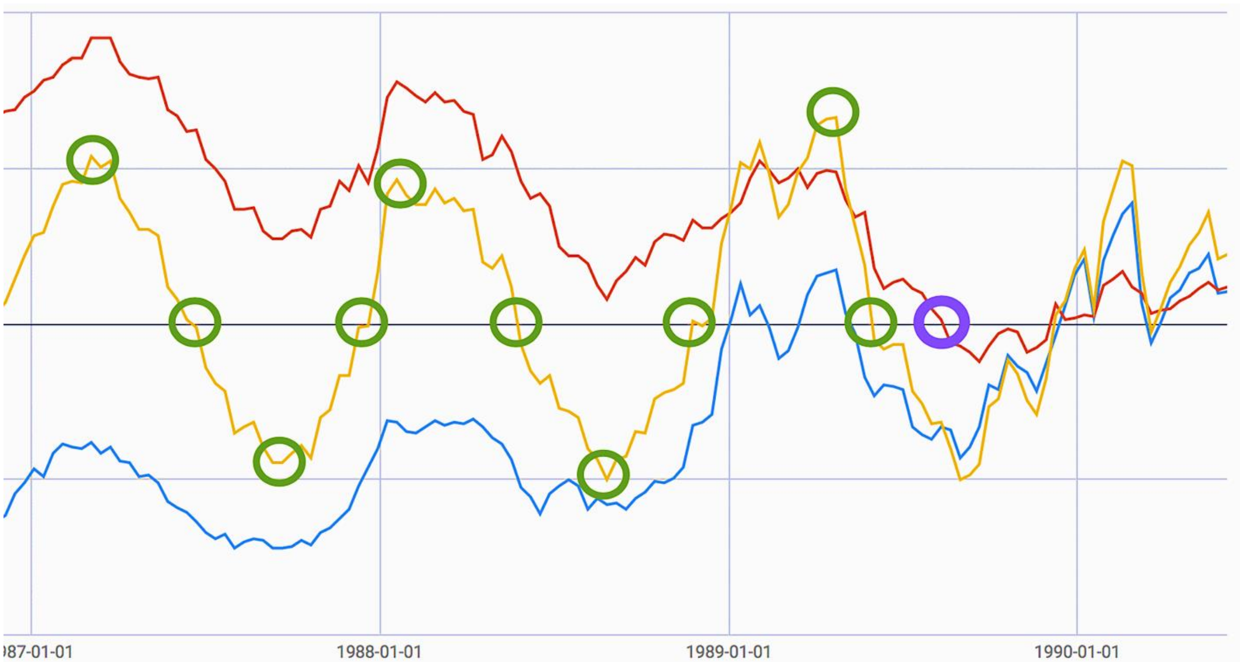


Figure 2: The N (blue), S (red) and N+S (yellow) SPF curves, with the significant SPF days during SPF maximum (green), and the beginning of a SPF reversal phase (purple) when both N and S SPF had made their first reversal of the cycle. Peaks and reversals during SPF reversal phase are excluded. In this ~1250-day segment of the dataset, there are 11 significant SPF days.

Manual confirmation of significant days was performed in duplicate. First, the significant points derived from the model were checked against the data in spreadsheet form. Separately, the peaks and reversals during SPF maximum were identified on a graphical representation of the SPF data (as in Figure 2), were subsequently checked against the spreadsheet to determine the dates of the points manually identified in the graph, and finally were compared to the model results both by hand and by common “compare documents” function in Microsoft Word. Upon complete agreement of the mathematical and manual methods as to identifying the significant SPF days in the entire data period, the simulations and analyses were performed. To determine if there is a relationship with the largest earthquakes, the significant SPF days were analyzed by real temporal correlation vs 10,000 random simulations generating 33 random dates within the time period (Jupyter). These 33 days would act as the “earthquake days” in the simulations, corresponding to the actual 33 M8+ earthquakes in the period, and their proximity in time to significant SPF days was statistically compared.

In addition to the simulations, the random distribution expectation is tested against the actual distribution of M8+ earthquakes.

## 4.0 Results

In 10,000 random simulations of earthquake days, the 33 simulated earthquake days were 41.63 days away from significant SPF days on average. The actual 33 M8+ earthquakes in the period averaged 33.0 days away, ~20% closer in time. In the simulations, an average of 7.7 earthquakes occurred within 10 days of significant SPF days, and an average of 4.9 within 5 days. Of the 33 real M8+ earthquakes, 16 occurred within 10 days of significant SPF days (>200% of simulation), and 9 occurred within 5 days (nearly 200% of simulation). Compared with the simulation, the correlation of actual M8+ events with significant SPF days fell in the 80$^{th}$ percentile in average days away, the 99.88$^{th}$ percentile in how many were within 10 days, and the 95.25$^{th}$ percentile in how many were within 5 days. An example of how the significant SPF days and actual M8+ earthquakes occur is shown in figure 3.

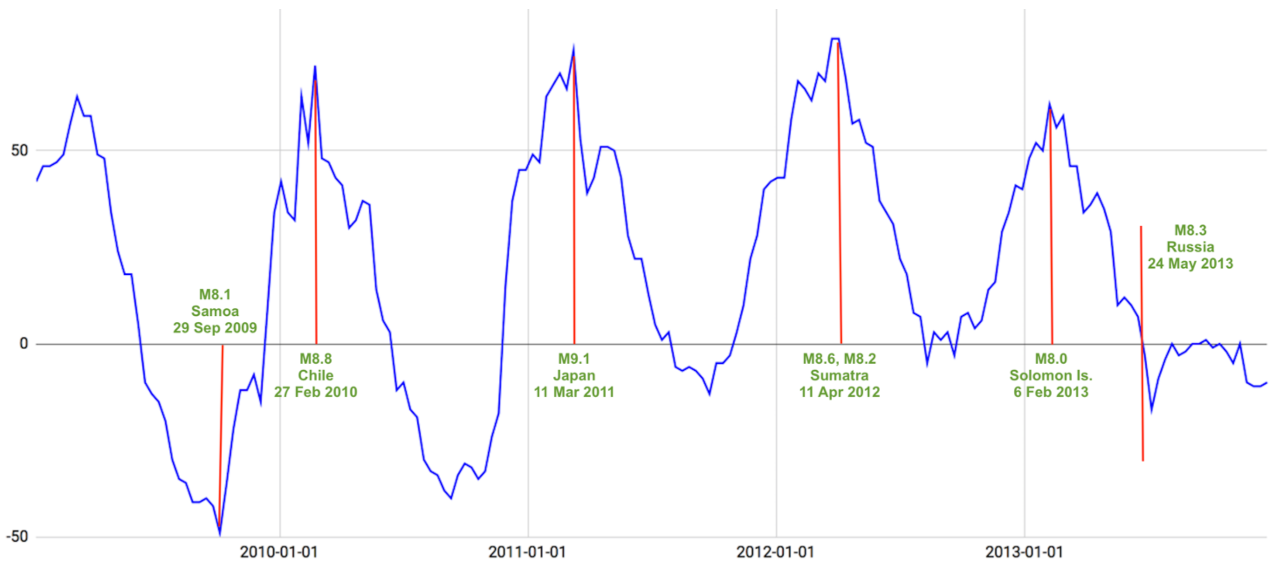


Figure 3: The N+S SPF from January 2009 through December 2013 (blue), where seven M8+ earthquakes occurred in the period (red). In sequential order, the earthquakes struck a negative maximum, then four straight positive maxima, and a reversal of SPF polarity. No other M8+ earthquakes occurred in the period.

The 5 largest earthquakes to occur during the total SPF data period occurred within 10 days from the significant SPF events in the model, and the largest 3 were within 5 days, as can be seen in Table 1.

| DATE | MAGNITUDE | LOCATION | DAYS-AWAY | SPF MOMENT |
|---|---|---|---|---|
| 11 Mar 2011 | 9.1 | Japan | 2 | + Peak |
| 26 Dec 2004 | 9.1 | Sumatra | 1 | N+S Reversal |

| | | | | |
|---|---|---|---|---|
| 27 Feb 2010 | 8.8 | Chile | 5 | + Peak |
| 11 Apr 2012 | 8.6 | Sumatra | 9 | + Peak |
| 28 Mar 2005 | 8.6 | Sumatra | 8 | + Peak |

Table 1: The largest five earthquakes in the data period are listed, with their date of occurrence, magnitude, location, and proximity to significant SPF moments (days).

This apparent correlation at the highest magnitude was subsequently tested in 100,000 additional simulations performed to test the frequency of the largest 5 events occurring within 10 days of significant SPF days, and the largest 3 events occurring within 5 days (Jupyter). 347 (0.347%) of simulations held the largest 5 events within 10 days, and 76 (0.076%) held the 3 largest events within 5 days. These results place the correlation of the actual M8+ events in the 99.65$^{th}$ and 99.92$^{nd}$ percentiles, respectively. The increasing proximity of M8+ occurrence and significant SPF days with increasing magnitude across the entire dataset can be seen in Figure 4.

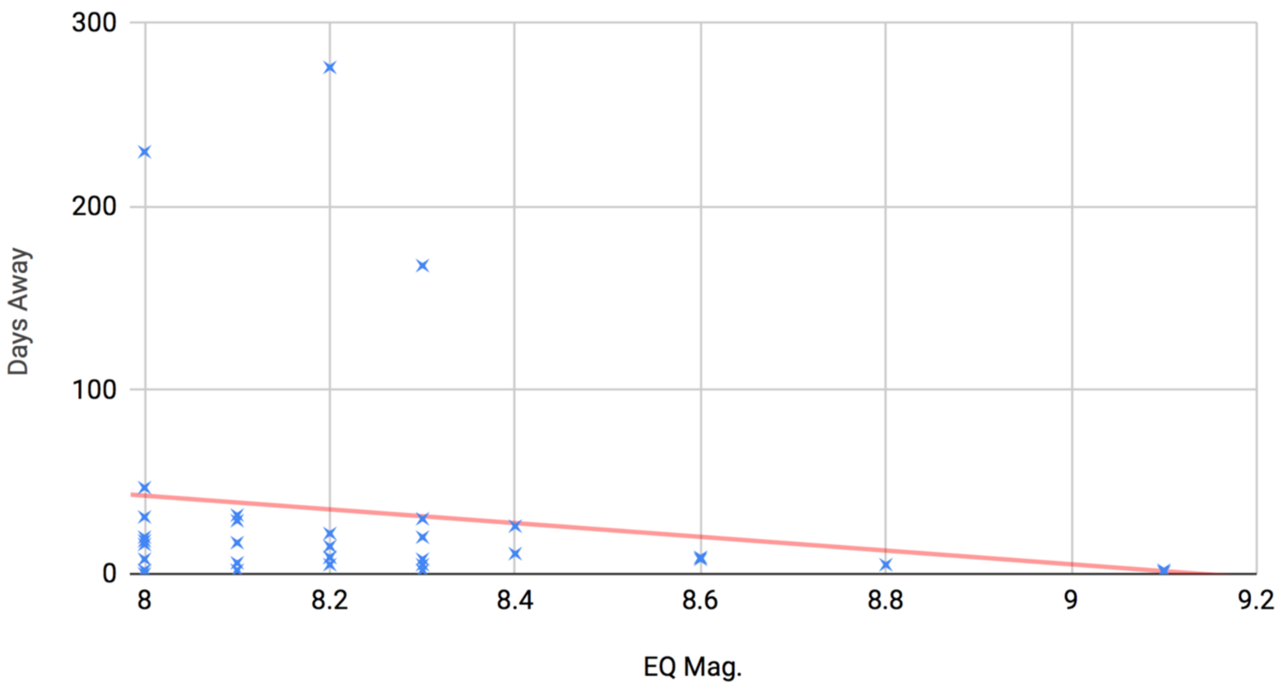


Figure 4: Each of the M8+ earthquakes is plotted along with the days away from significant SPF days (blue stars), showing a trend (red line) of increasing proximity with increasing magnitude.

The simulation results are comparable with expected statistical distributions. 213 significant SPF days distributed among the 1540 data points in the period produces and average of 7.23 data points (10-day averages), or 72.3 days between significant SPF days. Assuming 72 days between significant SPF days, the earthquakes should generally fall 0 and 36 days-away, with an average of 18 days. The simulation and the actual earthquakes were significantly worse than this expectation, but each instance had outliers that inflate the averages. For example, three of the actual M8+ earthquakes occurred 168, 230 and 276 days-away from Significant SPF days due to the exclusion of SPF reversal phase analysis in this study. Without these three outlier events, the average days-away from significant SPF days of the remaining 30 M8+ events is 13.83, 25% lower than expected, as opposed to 33 days-away with them included.

With an expected (random) average of 18 days-away, 16 or 17 earthquakes are expected to be within 18 or fewer days away. 10 days is 55.55% of 18 days, and so an expected 9.4 (.5555 x 17) of the total 33 M8+ events would be expected within 10 days based on random distribution. With an expected 28.48% (9.4/33) of the earthquakes occurring within 10 days of significant SPF days, the chances of fewer than 16 of the actual M8+ earthquakes occurred within 10 days is +98% $[P = {}^{n!}/_{k!(n-k)!}(p^k)(q^{n-k})]$. This binomial probability is indicative (2$\sigma$) of the temporal correlation implying increasing relevance of significant SPF days with the largest events.

## 5.0 Conclusion

The temporal correlations vs randomized simulations lend support to the concept that the earth's interaction with the SPF may be a part of the geophysical ensemble of pre-seismic processes at highest magnitude. In the 42 years since the start of the SPF dataset the M8+ earthquakes have occurred more closely in time than expected to the peaks in magnetism and reversals of polarity in the solar polar fields, especially in how many occurred within just 10 days of significant SPF days. The results of the simulations and randomness tests are compelling, and they support the previous results in Davidson et al. 2015.

## 6.0 Discussion

While it is well understood that electromagnetic phenomena precede, occur concurrently, and are evident after large seismic events, there is considerable debate as to what processes formally control these events. Similarly, here, there is a question of exactly how the SPF might play a role in the pre-earthquake processes, and why the correlation appears at the highest magnitude.

### 6.1 Possible Mechanisms of Action

The annual pattern of the SPF curve tends to bring maximum strength near the equinox, and polarity reversals near the solstice. These are appealing concepts; the fall/spring bring the maximum north/south heliographic latitude in orbital position, the fastest change of tilt relative to the sun, and therefore the largest change in angular velocity. Solstice periods represent maximum tilt of earth relative to the sun (angular velocity change reverses direction), as well as being earth's perihelion (January) and aphelion (July). These would imply strictly gravitational forcing mechanisms of these earthquakes, would be unlikely to produce electromagnetic pre-earthquake anomalies apart from known pre-earthquake processes, and would have only a spurious correlation with the Significant SPF days. The deviation of the earthquake days from the orbital variability events follows the deviations in Significant SPF days from those orbital events in thus study. Though appealing, the concept is not new, nor is it with a positive history of correlation.

The SPF themselves have little interaction with earth, but they are likely indicative of the IMF strength of the coronal holes to which earth's magnetosphere connects, and the character of the heliospheric current sheet at that heliographic longitude. Unlike the sun's electromagnetic radiation and charged particle emission (solar flares and CMEs, respectively), the interplanetary magnetic fields are *the only element of space weather that does not contend with earth's magnetic field* but instead couples and connects with the magnetosphere, and further allows direct particle exchange. Common examples of such exchanges are "flux transfer events" and "solar energetic particle" storms, which both involve energy bypassing the magnetosphere via interplanetary magnetic fields. Once this exchange occurs, the energetic fluctuations may have access to the lithosphere through the magnetosphere (L shells) and global electric circuit vertical column. The IMF and the current sheet are known to influence the induced currents in earth's atmosphere and ground.

Piezoelectric effects, pyroelectric effects (especially in subducted plates), charge transmission and domain re-arrangement due to thermoelectric effects and crystal deformation, electro-kinetic effects of water flowing in porous rock, and the capacitance properties of olivine, indicate the potential for electromagnetic stress to affect pre-earthquake processes. A change in the electromagnetic conditions can affect the temperature of the rock, and electrochemical changes at the fault contact area would be enhanced due to their intrinsic hydration and high conductivity. The changes to the contact area could weaken the material directly at the point of slip or thrust. In addition to direct application of current in the global circuit, the ULF to UHF frequencies produced at earth's surface by solar wind current sheet interaction with the magnetosphere are ubiquitous features at L-shell descent points into the earth. There is considerably more space weather interaction potential with the lithosphere than simply induced geomagnetic currents.

Any mechanistic processes would be cumulative with existing pressure dynamics due to known earthquake processes; it would not replace the proven processes. This cumulative effect would explain why the most-correlated events here were of excess magnitude.

## 6.2 Exogenous Pre-Earthquake Processes

The existence of an electromagnetic connection from the lithosphere to the sun, via the global and interplanetary electromagnetic systems, may suggest an expanded view of ongoing pre-seismic analyses and modeling, whereby space weather is currently used to exclude electromagnetic pre-seismic anomalies as being due to a solar process rather than the seismic stress. The temporal correlation may be more than coincident, and the epicenter-focused electromagnetic anomalies may be indicative of the now well-founded large-scale electromagnetic connection of the lithosphere-atmosphere-ionosphere.

Given the present analysis, the others indicating a relationship between the sun and earthquakes, the electromagnetic nature of both space weather and known pre-seismic anomalies, and the lithospheric access of the geomagnetic and geoelectric systems, there may be required a reconsideration of the independence of these events and variables. We suggest that the engagement of space weather with geophysical processes may be broader than commonly believed. The gravitational influences of earth as its distance, tilt, and angular velocity change may merit re-examination also. While a more-detailed analysis of those forcing pathways is outside the scope of this temporal study by independent methods, further research into exogenous influences over geophysical pre-earthquake processes is warranted.

Acknowledgements:
Authors extend tremendous appreciation to T. Hoeksema (Solar Physics, Stanford) for help in understanding their SPF data and the geophysical interactions with interplanetary magnetic fields. All data is freely available from Stanford's Wilcox Solar Observatory and the U.S. Geological Survey at the web addresses provided in both the text and the reference section (Stanford, USGS). Necessary materials for replication of the simulations are freely available in multiple downloadable formats from www.spaceweathernews.com/data-repository . A binomial probability calculator that can be used to perform the randomness expectation may be found here: http://vassarstats.net/binomialX.html .

There is no relevant funding for this study.

References:

Cataldi, D., Cataldi, G., Straser, V. (2017), SELF-VLF Electromagnetic Signals and Solar Wind Proton Density Variations that Preceded the M6.2 Central Italy Earthquake on August 24, 2016. *International Journal of Modern Research in Electrical and Electronic Engineering*, Vol. 19, EGU2017-3675, 2017

Davidson, B., U-yen, K., Holloman, C. (2015) Relationship Between M8+ Earthquake Occurrences and the Solar Polar Magnetic Fields. *New Concepts in Global Tectonics Journal*, V.3, No. 3, September 2015, pp. 311-323

Elfaki, H. & Yousef, S. (2017) A Proton Flare Triggered the Mw 8.1 Chiapas Mexican Earthquake. American Geophysical Union, Fall Meeting 2017, abstract #S33G-2955. http://adsabs.harvard.edu/abs/2017AGUFM.S33G2955E *accessed July 9, 2018*

Freund, F., Ouillon, G., Scoville, J., Sornette, D. (2017) Earthquake precursors in the light of peroxy defects theory: critical review of systematic observations. arXiv:

https://arxiv.org/abs/1711.01780 [physics.geo-ph], *(At time of access, July 13, 2018, manuscript has been accepted for publication in the European Physical Journal (EPJ) 2018)*

Guglielmi, A.V., Potapov, A.S. (2018) Do 5-minute Oscillations of the Sun affect the magnetosphere and lithosphere of the earth? arXiv: https://arxiv.org/pdf/1808.05367v1.pdf [physics.geo-ph]. Accessed August 1, 2018.

Hagen, M. & Azevedo, A. (2017) Possible Connections between X-Solar Flares and Worldwide Variation in Seismicity Enhancement. *Natural Science*, 9(12), 457-476. doi: 10.4236/ns.2017.912042

Jupyter, Python 2.7 code for present data analysis, available at www.spaceweathernews.com/data-repository

Larocca, P.A. (2016) Application of the Cross Wavelet Transform to Solar Activity and Major Earthquakes Occurred in Chile. *International Journal of Geosciences*, pp. 1310-1317. doi: 10.4236/ijg.2016.711095

Love, J.J., Thomas, J.N. (2013) Insignificant solar-terrestrial triggering of earthquakes. *Geophysical Research Letters*, 40(6), 1165-1170. doi: 10.1002/grl.50211

Marchetti, D., & Akhoondzadeh, M. (2018) Analysis of Swarm satellites data showing seismo-ionospheric anomalies around the time of the strong Mexico (Mw = 8.2) earthquake of 08 September 2017. *Advances in Space Research*, 62(3), 614-623. doi: 10.1016/j.asr.2018.04.043

Midya, S.K. & Gole, P.K. (2014) Trend of major earthquakes during the period 1900–2011 and its association with some solar and geomagnetic parameters. *Indian Journal of Physics*, 88(1) 1-4. doi: 10.1007/s12648-013-0369-2

Midya, S.K., Das, A., Karmakar, N. (2016) Association of occurrence of major earthquakes throughout the globe with variable component of the green line Fe XIV 530.3 nm during 1950–2014. *Indian Journal of Physics*, 90(12), 1341-1345. doi: 10.1007/s12648-016-0875-0

Odintsov, S., Boyarchuk, K., Georgieva, B., Kirov, B., Atanasov, D. (2006) Long-period trends in global seismic and geomagnetic activity and their relation to solar activity. *Physics and Chemistry of the Earth, Parts A/B/C*, 31(1-3), 88-93. doi: 10.1016/j.pce.2005.03.004

Ouzounov, D., Pulinets, S., Liu, J.Y., Hattori, K., Han, P. (2018) Multiparameter Assessment of Pre-Earthquake Atmospheric Signals. *Chapter 20*, Pre-Earthquake Processes (eds D. Ouzounov, S. Pulinets, K. Hattori and P. Taylor). American Geophysical Union, Geophysical Monograph Series (book series) doi:10.1002/9781119156949.ch20

Simpson, J.F. (1967) Solar Activity as a Triggering Mechanism for Earthquakes. *Earth and Planetary Science Letters*, 3, 417-425. doi: 10.1016/0012-821X(67)90071-4

Stanford University, Wilcox Solar Observatory; Solar Polar Magnetic Field Data Archive http://wso.stanford.edu/Polar.html *accessed July 20, 2018*.

Sukma, I. & Abidin, Z.Z. (2017) Study of seismic activity during the ascending and descending phases of solar activity. *Indian Journal of Physics*, 91(6), 595-606. doi: 10.1007/s12648-016-0943-5

Tavares, M., Azevedo, A. (2011) Influences of solar cycles on earthquakes. *Natural Science*, 3(6), 436-443. doi: 10.4236/ns.2011.36060

USGS; Earthquake Data Archive https://earthquake.usgs.gov/earthquakes/search *accessed July 20, 2018.*

Urata, N., Duma, G., Freund, F. (2018) Geomagnetic Kp Index and Earthquakes. *Open Journal of Earthquake Research*, 7(1), 39-52. doi: 10.4236/ojer.2018.71003

Velichkova T. & Kilifarska, N. (2018) Geomagnetic forcing of the lower stratospheric O3 and surface temperature short-term variability prior to earthquakes. *Sun and Geosphere*, 13(1), 7-13. ISSN: 2367-8852

Yu, X.X., Jin, C.L., An, Z.H. (2017) The Characteristics of Global Shallow-Source Seismicities Associated with Solar Activities in Different Time Scales. *Proceedings of Science*, 35th International Cosmic Ray Conference (Korea). PoS(ICRC2017)085. https://pos.sissa.it/301/085/pdf *accessed July 19, 2018.*